Received: 26 July 2017 | Revised: 6 March 2018 | Accepted: 8 March 2018

DOI: 10.1002/hbm.24050



RESEARCH ARTICLE

WILEY

# Degrees of functional connectome abnormality in disorders of consciousness

Dmitry O. Sinitsyn | Liudmila A. Legostaeva | Elena I. Kremneva | Sofya N. Morozova | Alexandra G. Poydasheva | Elizaveta G. Mochalova | Oksana G. Chervyakova | Julia V. Ryabinkina | Natalia A. Suponeva | Michael A. Piradov

Research Center of Neurology, 80 Volokolamskoe shosse, Moscow 125367, Russia

**Correspondence**
Dmitry O. Sinitsyn, Research Center of Neurology, 80 Volokolamskoe shosse, Moscow 125367, Russia.
Email: d_sinitsyn@mail.ru

**Funding information**
Russian Science Foundation, Grant/Award Number: 16-15-00274

## Abstract

Understanding the neuronal basis of disorders of consciousness can help improve the accuracy of their diagnosis, indicate potential targets for therapeutic interventions, and provide insights into the organization of normal conscious information processing. Measurements of brain activity have been used to find associations of the levels of consciousness with brain complexity, topological features of functional connectomes, and disruption of resting-state networks. However, obtainment of a detailed picture of activity patterns underlying the vegetative state/unresponsive wakefulness syndrome and the minimally conscious state remains a work in progress. We here aimed at finding the aspects of fMRI-based functional connectivity that differentiate these states from each other and from the normal condition. A group of 22 patients was studied (9 minimally conscious state and 13 vegetative state/unresponsive wakefulness syndrome). Patients were shown to have reduced connectivity in most resting-state networks and disrupted patterns of relative connection strengths as compared to healthy subjects. Differences between the unresponsive wakefulness syndrome and the minimally conscious state were found in the patterns formed by a relatively small number of strongest positive correlations selected by thresholding. These differences were captured by measures of functional connectivity disruption that integrate area-specific abnormalities over the whole brain. The results suggest that the strong positive correlations between the functional activities of specific brain areas observed in healthy individuals may be critical for consciousness and be an important target of disruption in disorders of consciousness.

**KEYWORDS**

consciousness, functional connectivity, magnetic resonance imaging, minimally conscious state, unresponsive wakefulness syndrome

## 1 | INTRODUCTION

Disorders of consciousness (DOC) constitute some of the most devastating neurological conditions. The extremely challenging task of improving the patients' state is further complicated by problems of diagnosis. The two aspects of normal consciousness—wakefulness and awareness—may become dissociated, which leads to the distinction between the state of preserved wakefulness without awareness, termed vegetative state (VS) or unresponsive wakefulness syndrome (UWS), and the state of wakefulness with minimal reproducible signs of awareness, known as the minimally conscious state (MCS) (Demertzi, Soddu, & Laureys, 2013). Practical differentiation between these states is challenging because subjective awareness of the environment cannot be measured directly but is instead evaluated by behavioral tests (Giacino, Fins, Laureys, & Schiff, 2014), which may underestimate the level of consciousness due to sensory, motor, or executive function impairments (Casarotto et al., 2016).

Problems of behavioral assessment of consciousness and the importance of correct diagnosis in rehabilitation and patient care decisions have led to an extensive search for objective methods of

  

evaluating the level of consciousness based on different modalities of brain activity measurement. The latter include positron emission tomography (PET) (Stender et al., 2014), functional magnetic resonance imaging (fMRI) (Demertzi et al., 2015; Wu et al., 2015), diffusion tensor imaging (DTI) (Zheng et al., 2017), and recording of electroencephalographic responses to transcranial magnetic stimulation (TMS-EEG) (Casali et al., 2013). These studies produced a number of important advances. The application of the TMS-EEG method resulted in the development of the perturbational complexity index (PCI), which was shown to successfully distinguish the states of consciousness in healthy individuals and to differentiate the UWS from higher levels of consciousness (Casarotto et al., 2016). PET measurements differentiated UWS and MSC patients with considerable accuracy (Stender et al., 2014). At the same time, there remains a significant proportion of borderline or anomalous cases where objective measurements diverge from each other or from clinical assessments (Bodart et al., 2017). Interpretation of such situations and understanding the difference in the aspects of consciousness measured by each method require further investigation.

Although the analysis of resting-state fMRI (rs-fMRI) data has initially shown a lower accuracy than PET in distinguishing UWS from MCS patients (Rosazza et al., 2016; Stender et al., 2014), this noninvasive and relatively fast method is a promising approach to provide information complementary to other measurements and could help disambiguate borderline cases. In addition, its lower cost and higher accessibility make it relevant for clinical application. Recently resting-state fMRI was applied for the discrimination between UWS and MCS, and the results coincided with the behavioral diagnosis using the Coma Recovery Scale-Revised in 20 of 22 patients (Demertzi et al., 2015).

Much of the research on functional connectivity in DOC has focused on the disruption of specific resting-state networks, especially the default mode network (DMN) (Heine et al., 2012; Rosazza et al., 2016; Vanhaudenhuyse et al., 2010). Within the DMN, the posterior cingulate cortex/precuneus (PCC/PCU) regions were identified as particularly important. Thus, in Wu et al. (2015), functional connectivity strength patterns predicted whether patients with unresponsive wakefulness syndrome/vegetative state and coma would regain consciousness with an accuracy of 81.25%, and the most discriminative region was the PCC/PCU. Along the same lines, Silva et al. (2015) showed that the correlation between posterior cingulate cortex and medial prefrontal cortex (also part of the DMN) in comatose patients predicted the Coma Recovery Scale-Revised (CRS-R) score 3 month after the scanning. More recent studies have also found disrupted connectivity in resting-state networks other than the DMN (Demertzi et al., 2014). Indeed, in the study (Demertzi et al., 2015), the highest accuracy of MCS/UWS classification was obtained using the auditory network, with the visual network and DMN rated second and third.

The findings of the studies attempting to distinguish between MCS and UWS suggest that this problem is more challenging than that of differentiating DOC patients from healthy controls, and the result is very sensitive to the type of analysis applied. Thus, the comparison of functional connectivity strength in Wu et al. (2015) revealed significant differences between DOC patients and controls, primarily in the default mode, salience and executive control networks; however, no significant difference between MCS and UWS was found. In Demertzi et al. (2014), the DMN and auditory network had the highest accuracy (85.3%) in discriminating patients from healthy subjects. At the same time, a significant difference between MCS and UWS was found only for the left executive control network when comparing the percentage of patients having the corresponding independent components of neuronal activity. Other networks did not show significant differences, and for the DMN this parameter was the same in MCS and UWS. Thus, further research is needed to identify methods of connectivity analysis that are most effective for solving this clinically important classification problem.

In addition to their clinical applications, studies of brain activity in DOC patients can provide important insights for the fundamental understanding of the neural basis of conscious information processing. In this regard, the complexity of normal neural signals, as revealed in the TMS-EEG responses by the PCI, highlighted the importance of integration and differentiation in the neuronal dynamics underlying consciousness (Casali et al., 2013). At the same time, many global network properties of functional connectomes of coma patients measured by fMRI showed no significant differences from those of healthy controls, whereas the connectivity of specific brain areas was substantially disrupted (Achard et al., 2012). These findings suggest that in addition to measures of overall brain dynamics, fine-grained location-specific analyses may be essential for the description of consciousness-supporting networks.

In this respect, recent advances in the evaluation of functional connectivity based on detailed brain parcellations into functionally homogeneous areas may prove helpful. The small size and special choice of the areas' locations increase the signal coherence of their voxels, which leads to more meaningful connectivity measures (Shen, Tokoglu, Papademetris, & Constable, 2013). Combining these atlases with the analysis that compares the individuals' connectomes in a node-specific way, but without restriction to a particular area or resting-state network, provides a tool sensitive to even small differences in the connectivity. This approach was successfully applied to several challenging problems, such as identification of an individual by their functional connectome (Finn et al., 2015) and prediction of performance in a sustained attention task based on fMRI data (Rosenberg et al., 2016). In the context of DOC research, the connectivity assessed by this method served as a basis for the recently developed ConnICA procedure providing a data-driven characterization of subjects at different levels of consciousness by the typical patterns in their connectomes (Amico et al., 2017).

In this study, we compared functional connectivity inferred from fMRI data in healthy individuals and in DOC patients in the MCS and UWS states. The goal was to determine the connectome features and the brain areas or networks in which the differences between the levels of consciousness were most prominent. We based our analysis on ROI-to-ROI connectivity matrices computed using a detailed fMRI-based atlas of brain areas (Shen et al., 2013). The resulting individual connectivity matrices were compared with the mean connectome of a reference group of healthy volunteers using the Pearson correlation. A similar analysis was applied to the strongest positive connections

**TABLE 1** Clinical characteristics of the enrolled patients

| ID | Sex | Age | Etiology | DOC duration, months | CRS-R total score | Diagnosis | Dexmedetomidine-induced sedation |
|---|---|---|---|---|---|---|---|
| 1 | M | 23 | TBI | 13 | 20 | MCS | + |
| 2 | M | 50 | Anoxia | 8 | 10 | MCS | + |
| 3 | M | 21 | Anoxia | 18 | 4 | UWS | − |
| 4 | F | 31 | Anoxia | 4 | 7 | UWS | − |
| 5 | F | 61 | Anoxia | 17 | 5 | UWS | − |
| 6 | F | 31 | Anoxia | 15 | 18 | MCS | + |
| 7 | M | 22 | Anoxia | 4 | 6 | UWS | − |
| 8 | M | 41 | Anoxia | 3 | 5 | UWS | + |
| 9 | F | 23 | TBI | 13 | 8 | UWS | − |
| 10 | M | 50 | Anoxia | 3 | 6 | UWS | − |
| 11 | F | 24 | TBI | 12 | 21 | MCS | + |
| 12 | M | 55 | Anoxia | 3 | 15 | MCS | + |
| 13 | M | 55 | Anoxia | 3 | 4 | UWS | − |
| 14 | F | 56 | Anoxia | 15 | 18 | MCS | − |
| 15 | M | 22 | TBI | 13 | 3 | UWS | − |
| 16 | F | 22 | TBI | 13 | 8 | UWS | − |
| 17 | M | 33 | TBI | 14 | 18 | MCS | + |
| 18 | F | 28 | Anoxia | 3 | 4 | UWS | − |
| 19 | M | 55 | Anoxia | 3 | 5 | UWS | − |
| 20 | F | 24 | Anoxia | 4 | 4 | UWS | − |
| 21 | M | 33 | Anoxia | 3 | 12 | MCS | + |
| 22 | M | 53 | Anoxia | 3 | 12 | MCS | − |

*Note*. Abbreviations: CRS-R = Coma Recovery Scale-Revised; F = female; M = male; MCS = minimally conscious state; TBI = traumatic brain injury; UWS = unresponsive wakefulness syndrome.

obtained by thresholding the connectivity matrices. The results were compared with the description at the level of nodal degrees using a variant of the hub disruption index introduced in Achard et al. (2012) and with the analysis of the total numbers of above-threshold connections. We also examined differences between subject groups in the mean connectivity within the commonly described resting-state networks.

## 2 | METHODS

### 2.1 | Subjects

Twenty-two patients (9 women, mean age 37 years, age range 21–61 years) admitted to the Research Center of Neurology, Moscow, Russia between 2014 and 2016 met the study inclusion criteria: chronic disorder of consciousness in permanent terms (at least 12 months since traumatic brain injury incident or at least 3 months since the episode of anoxia), no contraindications to MRI scanning, stable vital functions. Of them, 13 patients (59%) were diagnosed as being in a vegetative/unresponsive wakefulness state (VS/UWS), 9 patients (41%) in a minimally conscious state (MCS). Mean time since the incident was 13.0 months in traumatic brain injury patients ($n = 6$) and 6.8 months in DOC of anoxic etiology ($n = 16$). Table 1 summarizes the clinical characteristics of the enrolled patients.

Clinical assessment of consciousness was performed using the JFK Coma Recovery Scale-Revised (CRS-R), which comprises 23 hierarchically arranged items associated with brainstem, subcortical, and cortical processes (Giacino, Kalmar, & Whyte, 2004). The lowest item on each subscale represents reflexive activity, while the highest item represents cognitively mediated behaviors by addressing to auditory, visual, motor, oromotor, communication, and arousal functions. CRS-R is established as the most reliable tool for chronic DOC assessment (Seel et al., 2010). Validation of the Russian adaptation of the Coma Recovery Scale–Revised was conducted in Research Center of Neurology (Moscow) from October 2016 until April 2017, registered at clinicaltrials.gov (Identifier IDNCT03060317) (Mochalova et al., 2018). The CRS-R assessment was performed three times: on the day of fMRI, the day before, and the day after. The CRS-R scores and the MCS/UWS diagnoses were identical in the three evaluations.

Whenever possible, MRI acquisition was performed without sedation. However, to avoid motor artifacts during scanning in 8 patients (36%), an anesthesiologist induced light sedation by dexmedetomidine administration via intravenous infusion at a constant rate of 1 μg/kg/h. During the infusion period, the anesthesiologist monitored cuff blood pressure, electrocardiogram, and pulse oximetry.

In addition to DOC patients, we analyzed rest-fMRI data from two groups of healthy volunteers. The first group, referred to as the *reference group*, consisted of 14 healthy volunteers (6 women, mean age 40 years, age range 24–67 years) studied under the same protocol as the patients. The data for the second group, referred to as the *control group*, were taken from a publicly available dataset[1] from 20 healthy individuals (14 women, mean age 21 years, age range 18–26 years).

The analysis of two groups of healthy subjects was necessary for the following reasons. The main approach used here for the assessment of connectomes of patients was to compare them to the mean healthy connectome. The latter was obtained by averaging the connectomes of the first group of healthy volunteers, referred to as the *reference group*. The similarity of an individual's connectome to this mean connectome serves as a measure of its intactness. However, to establish a criterion of normality for this measure, we must estimate its distribution in the healthy population. An important caveat is that subjects from the reference group cannot be used for this estimation in an unbiased way because they are likely to be closer to the average of their group than any independent healthy individual. With this in mind, we used a dataset from a separate, independent group of healthy volunteers, referred to as the *control group*, to obtain unbiased estimates of the connectome intactness measures in the healthy population. The situation bears some analogy to that in supervised machine learning, where a *training set* (analogous to our reference group) is used to estimate the model parameters and a *test set* (similar to the control group here) provides an unbiased estimate of the model's accuracy.

The study was approved by the local ethical committee. Informed consent was obtained from the legal representatives of patients and from healthy volunteers before any study-related procedures.

## 2.2 | Data acquisition

The imaging protocol for the patient group and the reference group consisted of structural MRI acquisition (duration 9 min) and resting state fMRI (duration 7 min 36 s), so that the total time spent by the subjects in the scanner was 16 min 36 s. The scanning was performed in the afternoon to avoid confounds due to natural sleep rhythms. Imaging data were acquired using a Siemens MAGNETOM Verio 3 T clinical scanner with a standard 32-channel matrix head coil. Resting-state scans were acquired using a T2*-weighted echo planar (EPI) sequence (TE/TR = 30/2,400 ms, flip angle 90°, matrix 64 × 64; FoV 192 × 192 $mm^2$, 36 axial slices to cover the whole brain) with a voxel resolution of 3.0 × 3.0 × 3.0 $mm^3$. One fMRI scanning session was performed for each patient and control subject and consisted of 190 continuous resting state volumes. For spatial normalization and localization, a T1-weighted anatomical image was acquired (TE/TR = 2.47/1,900 ms, TI = 900 ms, flip angle 9°, matrix 256 × 256, FoV 250 × 250 $mm^2$, 176 sagittal slices to cover the whole brain) with an isotropic voxel resolution of 1.0 × 1.0 × 1.0 $mm^3$.

The acquisition parameters for the control dataset were TR = 3,000 ms, 47 contiguous slices, 119 volumes (total fMRI duration 5 min 57 s), matrix size 72 × 72, voxel size = 3.0 × 3.0 × 3.0 $mm^3$.

## 2.3 | Preprocessing

The data were processed using the CONN functional connectivity toolbox (Whitfield-Gabrieli and Nieto-Castanon, 2012), version 17b[2] and SPM12.[3] The preprocessing pipeline consisted of the following steps: realignment of functional images (motion correction), slice timing correction, coregistration, segmentation of structural data, normalization into standard stereotactic Montreal Neurological Institute (MNI) space, outlier detection/scrubbing using the artifact detection tool (ART[4]), and spatial smoothing with a Gaussian kernel of 8 mm. The number of outlier scans was checked to be less than half of all scans for every subject. Denoising was performed by removing the following confounders by linear regression: (a) the blood-oxygen-level dependent (BOLD) signal from the white matter and CSF masks (5 principal components of each signal); (b) scrubbing (as many regressors as identified invalid scans); (c) motion regression (12 regressors: 6 motion parameters + 6 first-order temporal derivatives). The resulting signals were band-pass filtered in the range 0.008–0.09 Hz.

## 2.4 | Connectivity analysis

### 2.4.1 | Index of connectome intactness

ROI-to-ROI connectivity analysis was performed using a detailed atlas of 278 brain areas constructed in Shen et al. (2013) as a result of optimization for functional homogeneity within the areas in healthy subjects.[5] The BOLD signal time course of every ROI was calculated. It consisted of 190 measurements repeated every 2.4 s (total duration 7 min 36 s) for the patients and the healthy reference group and of 119 measurements repeated every 3 s (total duration 5 min 57 s) for the healthy control group. The Fisher-transformed correlation coefficients between all pairs of these signals were computed, comprising a symmetric connectivity matrix (Figure 1). Its upper triangle (not including the diagonal elements) forms a connectivity vector.

The analysis of the disruption of functional connectomes was performed as follows. The connectivity vectors of the reference group of healthy volunteers were averaged to obtain the mean normal connectivity vector (Figure 1). The intactness of an individual connectome was assessed by computing the Pearson correlation coefficient of the individual connectivity vector with the mean normal connectivity vector. The Pearson correlation was used because it had previously been shown to be a useful measure of connectome similarity (Finn et al.,

[1]http://fcon_1000.projects.nitrc.org, Cambridge dataset (first 20 subjects)

[2]http://www.nitrc.org/projects/conn

[3]http://www.fil.ion.ucl.ac.uk/spm/

[4]http://www.nitrc.org/projects/artifact_detect

[5]https://www.nitrc.org/frs/?group_id=51

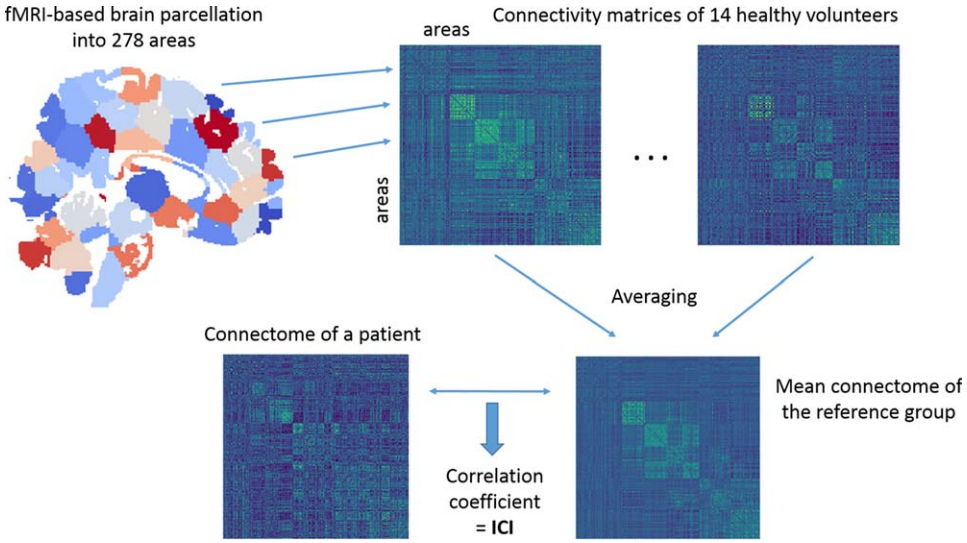


**FIGURE 1** Scheme of computation of the ICI index measuring the similarity of a patient's connectome to the mean connectome of the reference group of healthy subjects [Color figure can be viewed at wileyonlinelibrary.com]

2015). The resulting correlation coefficient is referred to below as the *index of connectome intactness (ICI)*.

### 2.4.2 | Index of thresholded connectome intactness

A similar analysis was performed taking into account only the strongest connections. All the connectivity vectors were thresholded at a given level, so that in the resulting vectors 0 corresponded to the correlations below the threshold and 1 to those above it. The average of the thresholded connectivity vectors from the reference group was computed. A component in this vector corresponding to a particular connection is equal to the frequency with which this connection passes the threshold in the connectomes of the reference group. This frequency serves as a measure of how typical it is of this connection to have a high positive value in a healthy individual. The correlation coefficient of the resulting vector with an individual thresholded connectivity vector was used as a measure of preservation of the strongest functional connections, termed *index of thresholded connectome intactness (ITCI)*.

### 2.4.3 | Hub disruption index

The above connectome analysis at the level of specific graph edges (connections) was compared with two other descriptions, based on nodal degrees and the total number of edges respectively. The first analysis employed a modification of the *hub disruption index (HDI)* introduced in Achard et al. (2012), computed as follows. The degrees of all nodes (i.e., numbers of connections of all brain areas; Wang, 2010) in the thresholded connectomes were found. For each subject in every group, a plot was produced with one point for each graph node. The *X* coordinate of a point was the mean degree of the node in the connectomes of the healthy subjects from the reference group, and the *Y* coordinate was the difference of the individual degree of the node in the current subject's connectome and its mean degree in the reference group. The hub disruption index was defined as the gradient of a straight line fitted to these points. If the hubs of healthy connectomes become nonhubs in a patient's connectome, then the HDI for this patient will have a negative value. For healthy subjects, the index should be relatively close to zero because the nodal degrees in healthy subjects' connectomes are expected to have considerable similarity. It should be noted that the above procedure of constructing the HDI has some deviations from the one defined in Achard et al. (2012). Thus, the Pearson correlation was used instead of wavelet correlation as a measure of connectivity to put the index in the same general framework with the other metrics considered, which are based on the Pearson correlation between BOLD signals. We also used a fixed threshold rather than a subject-specific threshold for choosing the strongest connections (in HDI as well as other thresholding-based characteristics), to extract correlations of similar statistical significance (see also the discussion in the Section 4.3).

The analysis at the level of nodal degrees can be viewed as a coarser description of connectomes than the previous edge-level analysis because there may exist a number of different graphs with the same set of nodal degrees (solutions to the so-called degree realization problem; Cloteaux, 2016), which would be discriminated by the ITCI but not the HDI.

### 2.4.4 | Number of suprathreshold connections

In the final (coarsest) type of analysis, the total numbers of suprathreshold connections were computed for every subject and compared between the groups.

### 2.4.5 | Connectivity within resting-state networks

The specificity of connectivity disruption to particular resting-state networks (RSNs) was studied as follows. The cortical parcellation into 7 networks from Yeo et al. (2011) was used.[6] Each of the 278 areas from the atlas was assigned to the resting-state network having the largest overlap volume with the area (or to no network if the largest overlap

[6]https://surfer.nmr.mgh.harvard.edu/fswiki/CorticalParcellation_Yeo2011

was with the space outside the RSNs). For each subject, we computed the average connectivity strength within each network defined as the mean correlation coefficient of all pairs of areas within the network. The distributions of the resulting numbers were compared between the control, MCS, and UWS groups.

### 2.5 | Statistical analysis

The above metrics of connectome disruption were compared between the subject groups using the Mann–Whitney test, which is robust to outliers. In addition to the probability value, we report the effect size computed as the Mann–Whitney statistic divided by the product of the sample sizes. This measure is known under several names: probability of superiority, common language effect size, and area under receiver operating characteristic curve (AUC). It estimates the probability with which a random value from the first population will be greater than a random value from the second one. Confidence intervals for ES were computed using the R package pROC (Robin et al., 2011).

The possible effects of the covariates (age, gender, etiology, sedation and DOC duration) along with the effect of interest (diagnosis of MCS or UWS) on the ITCI and HDI within the patient group were approximately tested using robust rank-based estimation and inference for an additive general linear model as described in Hettmansperger and McKean (2011) and Hollander and Wolfe (1999) and implemented in the package Rfit[7] (Kloke and Mckean, 2012).

It is important to note that the metrics based on the mean healthy connectome (ICI, ITCI, HDI) were compared between the patient group and the independent healthy control group, which was not used in the averaging (see also the rationale for using two healthy groups in Section 2.1). Thus, a significant effect found in such a comparison does not merely say that there is some difference between the patients and the subjects by which the average was computed (i.e., the reference group). Instead, it shows that this difference is significantly greater than that expected for a randomly taken healthy individual, presumably indicating an abnormality in the patients' connectomes. We also used other metrics that characterize an individual connectome on its own, without reference to any averaged data (total number of suprathreshold connections, mean connection strengths within resting-state networks). Unlike the previously mentioned measures, these parameters are not tied to the reference group, and we expect them to have no bias in this group compared to the general healthy population. Thus, we compared such metrics between the patient group and the healthy reference group, as this group was studied under an identical protocol and thus provided the most accurate benchmark for these parameters.

The choice of the connection threshold value is an important aspect in all the connectome characteristics that involve thresholding (ITCI, HDI, number of total suprathreshold connections). This value determines the minimal value of correlations that are analyzed, and can be chosen to provide better sensitivity to the relevant connectome features. However, if a result depends on the threshold being confined to a narrow range of values, such a result is more likely to be a false positive and not generalize to the whole population. For this reason, we conducted sensitivity analyses checking if the results are robust to the change of the threshold within an interval of a reasonable size. To avoid overfitting, we did not optimize the threshold value for the best separation of the studied groups of individuals. Rather, we report the results of statistical tests for an arbitrary threshold value in the range where there is a significant effect. It should be kept in mind that the specific reported empirical probability values and effect size estimates are subject to variability. The latter is due to variations of connection strengths in the populations and their relationship to the correlation threshold chosen.

[7]https://cran.r-project.org/package=Rfit

## 3 | RESULTS

A summary of the results is given in Table 2.

### 3.1 | Index of connectome intactness

The distributions of the index of connectome intactness (ICI) in healthy controls and DOC patients were significantly different (Figure 2). However, the ICI did not differ significantly between the UWS and MCS patient groups (data not shown).

### 3.2 | Index of thresholded connectome intactness

A significant difference between MCS and UWS patients, as well as between patients and controls, was found in the index of thresholded connectome intactness (ITCI, Figure 3a,b), with patients in MCS having higher (closer to normal) ITCI values than in UWS. The distributions for MCS and UWS were significantly different ($p < .05$, Mann–Whitney test) for all threshold values between 0.4 and 1.1. An arbitrary threshold value in this range (1.0) was chosen for illustrating the effect in Figure 3a. The estimated effect size (probability of superiority, or AUC) is 0.88 (95% CI: 0.74, 1). Choosing a reasonable critical value of $ITCI^* = 0.089$ and classifying patients with $ITCI > ITCI^*$ as MCS and as UWS otherwise, one obtains a specificity of 0.77 (95% CI[8]: 0.46–0.94) and a sensitivity of 0.89 (95% CI: 0.51–0.99) for detecting MCS.

### 3.3 | Hub disruption index

The hub disruption index (HDI) measures the deviation of the nodal degrees in a subject' connectome from their mean values in the reference group. Similar to the ITCI, the HDI showed a significant difference between MCS and UWS (Figure 4a, Mann–Whitney test, $p < .05$ for all thresholds above 0.8), with MCS having larger (closer to normal) HDI values. In healthy controls, the HDI was higher than in both patient groups.

### 3.4 | Number of suprathreshold connections

The comparison of the total numbers of suprathreshold connections demonstrated that these numbers were similar in the MCS and UWS

[8]Confidence interval calculated according to the efficient score method (Newcombe, 1998), http://vassarstats.net/clin1.html

**TABLE 2** Group comparisons of connectome characteristics

| # | Measure | Healthy versus DOC; sample sizes: 20, 22 (rows 1–3), 14, 22 (rows 4,5) | MCS versus UWS; sample sizes: 9, 13 |
|---|---|---|---|
| 1 | Index of connectome intactness (ICI), Figure 2 | Greater for healthy<br>$p = 7 \times 10^{-11}$<br>ES = 0.99 (95% CI: 0.97, 1) | No significant difference<br>$p > .05$ |
| 2 | Index of thresholded connectome intactness (ITCI) (threshold = 1), Figure 3 | Greater for healthy<br>$p = 2 \times 10^{-11}$<br>ES = 0.99 (95% CI: 0.98, 1) | Greater for MCS<br>$p = .002$<br>ES = 0.88 (95% CI: 0.74, 1) |
| 3 | Hub disruption index (HDI) (threshold = 1), Figure 4a | Greater for healthy<br>$p = 10^{-8}$<br>ES = 0.95 (95% CI: 0.9, 1) | Greater for MCS<br>$p = .04$<br>ES = 0.77 (95% CI: 0.53, 1) |
| 4 | Total number of suprathreshold connections (threshold = 1), Figure 4b | Greater for healthy<br>$p = 6 \times 10^{-4}$<br>ES = 0.85 (95% CI: 0.71, 0.99) | No significant difference<br>$p > .05$ |
| 5 | Mean connection strengths in resting-state networks, Figure 5 | Greater for healthy<br>$p < .05$ (Holm–Bonferroni corrected) for all networks except Limbic | No significant difference<br>$p > .05$ |

Two-tailed $p$ values of the Mann–Whitney test are indicated. ES: effect size defined as the Mann–Whitney statistic divided by the product of the sample sizes. This measure is known under several names: probability of superiority, common language effect size, area under receiver operating characteristic curve (ES = AUC). It estimates the probability with which a random value from the first population will be greater than a random value from the second one.

groups (Figure 4b). At the same time, healthy controls had a larger number of strong positive connections than patients did (Mann–Whitney test, $p < .001$ for all threshold values in Figure 4b).

## 3.5 | Connectivity within resting-state networks

The distributions of mean connection strengths (Fisher-transformed correlation coefficients) between areas in each resting-state network for healthy volunteers and DOC patients are shown in Figure 5. They were significantly different (after the Holm–Bonferroni correction) for all the networks except the Limbic one. A similar comparison between MCS and UWS showed no significant difference in the mean connection strengths within resting-state networks (data not shown).

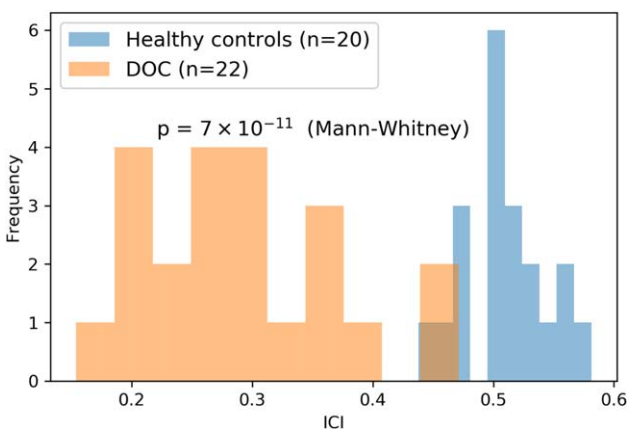


**FIGURE 2** Distributions of the index of connectome intactness in healthy controls and DOC patients. Here and below two-tailed $p$ values are indicated. Effect size is given in Table 2. Note that here and in Figures 3a,b and 4a, an independent healthy control group is used to obtain an unbiased estimate of a healthy individual's connectome similarity to the mean connectome of the reference group [Color figure can be viewed at wileyonlinelibrary.com]

## 3.6 | Effects of covariates

The effects of the covariates (age, gender, etiology, sedation and DOC duration) and the parameter of interest (diagnosis of MCS or UWS) on the ITCI and HDI within the patient group were approximately tested using rank-based estimation and inference for an additive general linear model. There were two pairs of significantly correlated covariates: (a) etiology and DOC duration (on average, longer for TBI), (b) sedation and diagnosis (MCS patients showed a tendency for greater motion and thus received sedation more often than those in UWS). This circumstance, known as multicollinearity (Öztürk and Akdeniz, 2000), makes regression unstable, and thus we included only one regressor from each pair, the whole set of factors consisting of age, gender, etiology, and diagnosis. For both the ITCI and the HDI (computed at the threshold level 1.0), the only significant predictor was the diagnosis ($p = 5 \times 10^{-4}$ and 0.03, respectively). The fraction of rank-based dispersion explained by the model (robust $R^2$; Kloke and Mckean, 2012) was 0.5 and 0.24, respectively, for the ITCI and the HDI. Distinguishing the effects of the correlated predictors requires further study (discussed below).

# 4 | DISCUSSION

## 4.1 | Differences between the states of consciousness in the whole-brain connectivity metrics

In this study, we have analyzed the functional connectomes of patients in chronic MCS and UWS as a result of trauma or anoxia in comparison with healthy individuals. The goal was to capture the patterns of abnormal connectivity, starting at a relatively high level of topographical detail, with minimal a priori assumptions, and checking whether the abnormalities would also be manifest at coarser levels of description and would be specific to certain locations and resting-state networks. This allowed us to find several connectome characteristics that distinguish the levels of consciousness and may thus be important for

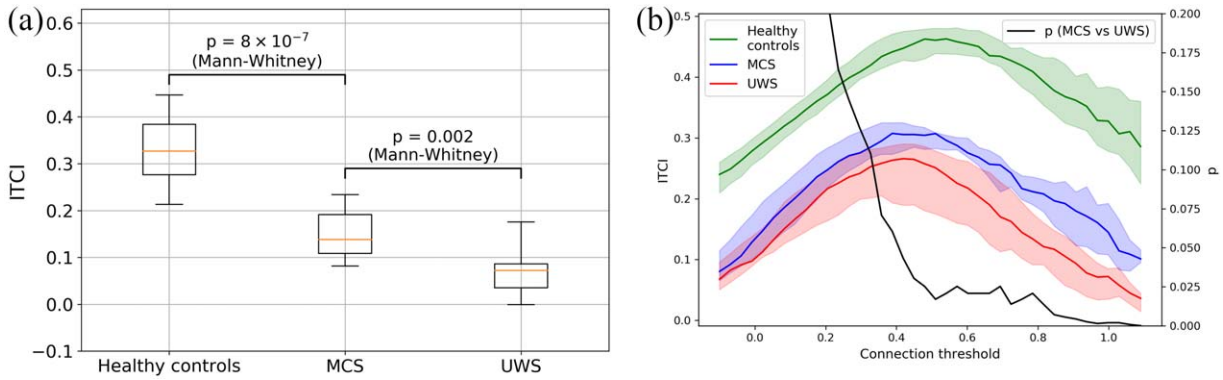


**FIGURE 3** (a) Distributions of the index of thresholded connectome intactness in healthy controls, MCS, and UWS patients. Boxes correspond to interquartile ranges, whiskers to ranges, and horizontal lines to medians. The threshold value is 1.0 (applied to Fisher-transformed correlation coefficients). Effect sizes are given in Table 2. (b) Sensitivity to the threshold value of the difference in ITCI between MCS and UWS patients. The lines with shadings show the medians and the interquartile ranges of ITCI in each group as a function of the threshold. Black line without shading: *p* values of the Mann–Whitney test between the MCS and UWS groups (secondary *y*-axis) [Color figure can be viewed at wileyonlinelibrary.com]

conscious information processing, including the features presumably underlying the limited conscious experiences distinguishing MCS patients from those in UWS.

First, we evaluated the connectivity using the index of connectome intactness (ICI) that was introduced to capture the similarity of an individual connectome to the mean connectivity pattern of the reference group of healthy volunteers. An advantageous property of this measure is that it is not constrained by any a priori hypotheses regarding either the locations or the specific character of the differences expected. Thus, compared to a systematic search over a range of features, the ICI does not suffer from loss of power due to multiple comparisons. However, the application of the index is based on the assumption that the reference group's connectomes, represented as points in the multidimensional connectome space, are concentrated around their mean point, and the groups compared by the ICI differ in their mean distance from this point. This turned out to be true for the healthy control and patient groups, where a highly significant difference in the index was found, with only a small overlap of the distributions (Figure 2). The same did not hold for the UWS and MCS groups. A tentative explanation of this is that the differences between the two patient groups are more subtle, and may be limited to a subset of connectivity dimensions and thus concealed by the majority of connections that are similar in their abnormality.

A similar analysis was performed after limiting the comparison to the set of the strongest positive correlations obtained by thresholding. The motivation for this is partly that large correlation coefficients can be estimated with a greater relative accuracy from the limited number of fMRI scans, and partly that strong correlations may be more likely to indicate genuine functional relatedness of the areas and thus be more physiologically meaningful. The resulting measure of similarity of an individual thresholded connectome to the mean one for the reference group, termed the index of thresholded connectome intactness (ITCI), was found to successfully differentiate the MCS and UWS patients at the group level (Figure 3). It also showed a highly significant difference between healthy controls and patients as a whole. The significance of the difference between the MCS and UWS groups was moderate, but robust to the choice of the threshold value in the range from 0.4 to 1.1. This result indicates that the patterns of strong positive connections in MCS patients are moderately, but significantly closer to their normal counterparts than those in the UWS group.

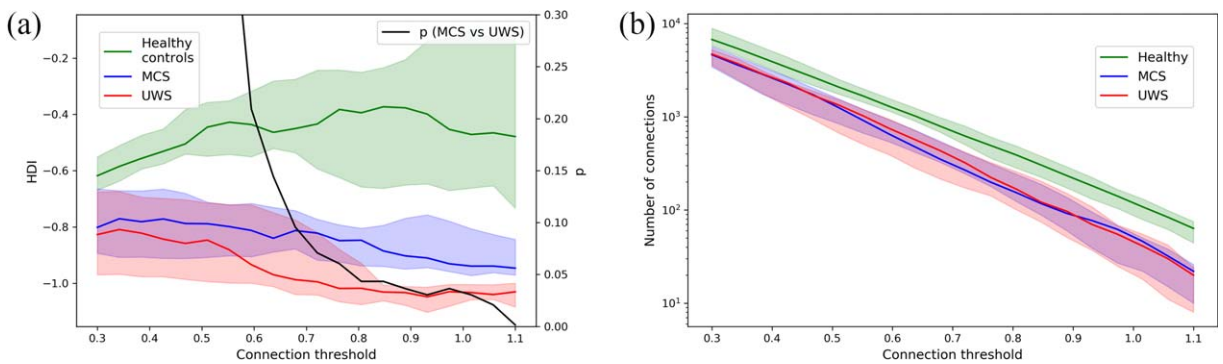


**FIGURE 4** (a) Distributions of the hub disruption index in the subject groups depending on the threshold. The lines with shadings show the medians and the interquartile ranges. Black line without shading: *p* values of the Mann–Whitney test between the MCS and UWS groups (secondary *y*-axis). (b) Distributions of the number of suprathreshold connections. Effect sizes are given in Table 2 [Color figure can be viewed at wileyonlinelibrary.com]

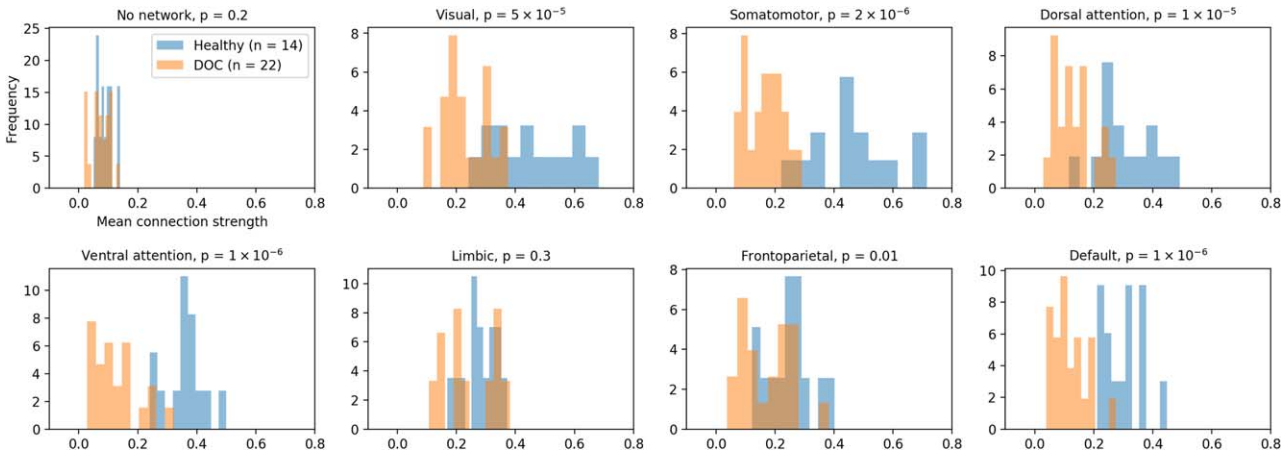


**FIGURE 5** Distributions of mean connection strengths within resting-state networks for DOC patients and healthy subjects (reference group). Top left: connections between areas not assigned to any network. Uncorrected *p* values of the Mann–Whitney test are indicated. For all the networks except the Limbic, the differences remain significant after the Holm–Bonferroni correction [Color figure can be viewed at wileyonlinelibrary.com]

We also explored the differences in the coarser aspects of thresholded connectome topology, specifically, the degrees of the nodes and the total number of edges. A modification of the hub disruption index from Achard et al. (2012) was used to test if there was a significant difference in the sets of hub nodes between MCS and UWS. Similar to the ITCI, this analysis showed a moderately significant increase in the HDI index in MCS compared to UWS patients, as well as substantially higher values of the index in healthy controls than in patients (Figure 4a). These results show that the HDI, which initially was shown to differentiate coma patients from healthy subjects (Achard et al., 2012), is also sensitive to the presumably smaller abnormalities in the connectomes of awake DOC patients and to the even more subtle differences between the MCS and UWS subgroups. One of the implications of this is that MCS patients have a greater number of conserved normal hub nodes than UWS patients. The corresponding brain areas may serve as candidate targets for noninvasive stimulation aimed at improving the patients' condition.

The coarsest type of whole-connectome analysis we applied was based on the total numbers of edges in the thresholded connectomes. These were similar for the MCS and UWS groups, but significantly higher in healthy controls than in patients (Figure 4b). This implies that the general level of connectivity in DOC patients is reduced, at least as regards strong positive connections, compared to healthy volunteers. At the same time, the two patient groups differ in the exact locations of the connections but not in their total number. This suggests that the general level of functional connectivity is not sufficient to explain the differences in the individual levels of consciousness, and some aspects of normal information processing require the presence of certain topography-specific patterns of correlations. As the strength of connectivity may be conceptually related to functional integration in brain networks discussed in Casali et al. (2013), an interesting question for further investigation is whether the above findings correspond to MCS patients having similar integration, but higher differentiation than subjects in UWS. It should be remembered, however, that the integration probed in Casali et al. (2013) by TMS-EEG may be different from the one derived from rs-fMRI. TMS-EEG captures effective connectivity while rs-fMRI-based functional connectivity is correlational, and measured on a larger timescale, and so the relationship between them is largely an open question (Fox et al., 2012).

Several other recent studies attempted to predict the MCS and UWS diagnosis based on different types of biomarkers from PET, DTI, EEG, and fMRI data and showed promising results, reviewed in Noirhomme, Brecheisen, Lesenfants, Antonopoulos, and Laureys (2017). Due to limited sample sizes, the confidence intervals for sensitivity and specificity are wide and overlap considerably. Thus, to draw definite conclusions about the relative accuracy of the different approaches, including the one presented here, further research on larger samples is necessary.

It is important to note that one of the most promising methods, the perturbational complexity index (PCI) derived from TMS-EEG, has better specificity and sensitivity for MCS/UWS (Casali et al., 2013; Casarotto et al., 2016) than those shown here by both ITCI and HDI. The differences reported above are group-level effects, whereas PCI can work at the single-subject level. Further research is needed to test whether data from these approaches can be combined to increase the accuracy of DOC diagnosis.

## 4.2 | Differences in the connectivity within resting-state networks

In addition to whole-brain characteristics, we investigated whether there were differences between the subject groups in the connectivity within specific resting-state networks. The more prominent contrast between healthy controls and DOC patients as a whole was significant in the default, ventral attention, somatomotor, dorsal attention, visual, and frontoparietal networks. The MCS and UWS groups did not show significant differences in this analysis. Although in previous studies these groups were reported to be different in certain features of functional connectivity in specific resting state networks (Demertzi et al., 2014, 2015; Rosazza et al., 2016), the effects and the relative

importance of the networks are sensitive to the type of analysis applied. The present comparison suggests that a simple measure of connectivity equal to the mean correlation of ROIs in a network can capture the differences between healthy subjects and DOC patients, but not between MCS and UWS. A similar finding was reported for functional connectivity strength (Wu et al., 2015), which measures the total connectivity of an individual voxel with the whole brain. This suggests that the subtle contrast between MCS and UWS may require more intricate analysis methods.

The observed effects in the Visual and Somatomotor networks are in line with the fact that in the recently developed ConnICA method (Amico et al., 2017), the so-called VIS-SM (visual and sensory motor) connectome component was one of the two traits (along with the fronto-parietal-DMN) that showed significant associations with clinical measures of awareness. The default network has probably been the most frequently reported system having abnormalities in DOC patients (Rosazza et al., 2016; Soddu et al., 2012; Vanhaudenhuyse et al., 2010). However, in accordance with recent reports (Demertzi et al., 2015), the above findings suggest that disorders of consciousness are associated with a massive disruption of most of the brain's functional networks, with only a moderate, and possibly subject-dependent, specificity to particular systems.

### 4.3 | Methodological issues

The study has several limitations. The presence of substantial structural damage and enlarged ventricles in a number of patients may have reduced the accuracy of image normalization, which could have led to artifacts in the connectivity analysis. Although the development of improved methods for normalizing lesioned brains is an area of active research (Andronache et al., 2013; Crinion et al., 2007; Ripollés et al., 2012), they are still far from eliminating the problem. Exclusion of patients with substantial anatomical distortions was not feasible due to limited sample size. Moreover, this approach is not ideal as it is likely to introduce bias into conclusions about the whole DOC population. Thus, we relied on manually checking that the normalization produced reasonable results. The remaining inaccuracies, however, may have been one of the factors precluding precise individual prediction of clinical state by functional connectivity.

The mean connectome of healthy subjects, used in the construction of the connectivity indices (ICI, ITCI, and HDI), was estimated from the reference group. This implies the identity of the notion of the "norm" with the average data from the subjects in this group. However, the medical norm may be or not be equal to the statistical norm. This problem is ubiquitous and cannot be solved as long as we do not have a definition of the medical norm.

The regression analysis of the effects of the covariates was limited in power by the sample size and by the presence of correlated predictors: (a) etiology and DOC duration, (b) sedation and diagnosis. It has been reported that dexmedetomidine reduces average brain connectivity strength in healthy individuals (Hashmi et al., 2017), although its effect on some aspects of brain connectivity was found to be smaller than that of propofol and non-rapid-eye-movement sleep (Guldenmund et al., 2017). These results suggest that the effect of sedation may be significant in our context. We note, however, that in this study sedation was applied mostly to MCS patients (due to their higher propensity to motion during scanning), and it is reasonable to assume that their connectomes without sedation would be even closer to normal, and thus the differences between the MCS and UWS groups would be more pronounced than reported here. Comprehensive characterization of the effects of the subject parameters on measures of functional connectome abnormality requires further investigation. It is also interesting to compare the results with (Amico et al., 2017) where age and gender were found not to be significant predictors of the most prominent functional connectome traits (similarly to the present analysis), whereas sedation, etiology, disease duration, and clinical state explained some of the variance in those traits.

The threshold for binarizing connectivity matrices can be chosen in a number of ways, the two most common of which employ a fixed threshold value and a subject-dependent one producing a given number of edges (or connection density) (van den Heuvel et al., 2017). For patients with lowered overall functional connectivity the former approach leads to sparser graphs than for healthy controls, whereas the latter includes lower correlations that are more likely to be spurious, which can lead to artefactual topological differences between subjects' connectomes (van den Heuvel et al., 2017). We used a fixed threshold to extract functional correlations of comparable strength and statistical significance. At the same time, because there was a significant difference in the overall connectivity in healthy subjects and DOC patients (Figure 4b), the contrast between these groups in the other thresholding-based metrics may have been a consequence of this fact. However, the comparison using the ICI does not involve thresholding and shows the differences in the relative connection strengths. Thus, the abnormalities in DOC patient's connectomes are not limited to the overall reduction in functional correlations, but consist instead in a reorganization of their patterns with respect to the healthy subjects' data. Similarly, the comparison of the MCS and UWS groups showed a difference in connection patterns, whereas the overall connectivity was similar.

## 5 | CONCLUSIONS

The results of this study show that the differences in functional connectomes of DOC patients and healthy subjects are substantial, and can be observed at different levels of coarseness of description: from the overall connectivity strength, to the numbers of connections of particular brain areas (nodal degrees), to the disruption of specific functional correlations. DOC patients were shown to have lower connectivity across most resting-state networks, with large differences in the default, ventral attention, somatomotor, dorsal attention, visual, and frontoparietal networks.

The contrast between the minimally conscious and unresponsive wakefulness syndrome patients was more subtle and not observable at the level of overall connectivity. Significant differences were found in the patterns of strong positive connections using node-specific whole-

brain measures of connectome disruption. One of them was the here introduced index of thresholded connectome intactness measuring the similarity of an individual pattern of strongest correlations to the corresponding mean pattern in healthy subjects. The other metric was a modified version of the hub disruption index (Achard et al., 2012) capturing the diminished connectivity of the areas that were high-degree hub nodes in healthy connectomes.

The results of this study suggest that the abnormalities in DOC patients' functional connectivity, and specifically in UWS compared to MCS, are most prominent in the strongest positive ROI-to-ROI correlations. Additionally, it is not just the absolute number of such connections that is likely to be important for consciousness, but also the particular pattern of strong correlations between specific regions.

Further research, including theoretical models, is needed to understand the possible role of the normal connectivity patterns in conscious information processing and the connection of the here quantified graded disruptions of these patterns to the observed functional deficits in DOC patients.

### ACKNOWLEDGMENTS

This study was supported by the Russian Science Foundation under grant 16-15-00274.

The authors thank Alina Guseva for the linguistic revision of the article.

## COMPETING INTERESTS

The authors declare that they have no competing interests.

### ORCID

*Dmitry O. Sinitsyn* http://orcid.org/0000-0001-9951-9803
*Elena I. Kremneva* http://orcid.org/0000-0001-9396-6063
*Sofya N. Morozova* http://orcid.org/0000-0002-9093-344X

### REFERENCES

Achard, S., Delon-Martin, C., Vértes, P. E., Renard, F., Schenck, M., Schneider, F., … Bullmore, E. T. (2012). Hubs of brain functional networks are radically reorganized in comatose patients. *Proceedings of the National Academy of Sciences of the United States of America*, *109* (50), 20608–20613.

Amico, E., Marinazzo, D., Di Perri, C., Heine, L., Annen, J., Martial, C., … Goñi, J. (2017). Mapping the functional connectome traits of levels of consciousness. *NeuroImage*, *148*, 201–211.

Andronache, A., Rosazza, C. P., Sattin, D. P., Leonardi, M. M., D'incerti, L. M., Minati, L., & Coma Research Centre (CRC) – Besta Institute. (2013). Impact of functional MRI data preprocessing pipeline on default-mode network detectability in patients with disorders of consciousness. *Frontiers in Neuroinformatics*, *7*, 16.

Bodart, O., Gosseries, O., Wannez, S., Thibaut, A., Annen, J., Boly, M., … Laureys, S. (2017). Measures of metabolism and complexity in the brain of patients with disorders of consciousness. *NeuroImage: Clinical*, *14*, 354–362.

Casali, A. G., Gosseries, O., Rosanova, M., Boly, M., Sarasso, S., Casali, K. R., … Massimini, M. (2013). A theoretically based index of consciousness independent of sensory processing and behavior. *Science Translational Medicine*, *5*(198), 198ra105–198ra105.

Casarotto, S., Comanducci, A., Rosanova, M., Sarasso, S., Fecchio, M., Napolitani, M., … Massimini, M. (2016). Stratification of unresponsive patients by an independently validated index of brain complexity. *Annals of Neurology*, *80*(5), 718–729.

Cloteaux, B. (2016). Fast sequential creation of random realizations of degree sequences. *Internet Mathematics*, *12*(3), 205–219.

Crinion, J., Ashburner, J., Leff, A., Brett, M., Price, C., & Friston, K. (2007). Spatial normalization of lesioned brains: Performance evaluation and impact on fMRI analyses. *NeuroImage*, *37*(3), 866–875.

Demertzi, A., Antonopoulos, G., Heine, L., Voss, H. U., Crone, J. S., De Los Angeles, C., … Laureys, S. (2015). Intrinsic functional connectivity differentiates minimally conscious from unresponsive patients. *Brain*, *138*(Pt 9), 2619–2631.

Demertzi, A., Gómez, F., Crone, J. S., Vanhaudenhuyse, A., Tshibanda, L., Noirhomme, Q., … Soddu, A. (2014). Multiple fMRI system-level baseline connectivity is disrupted in patients with consciousness alterations. *Cortex*, *52*, 35–46.

Demertzi, A., Soddu, A., & Laureys, S. (2013). Consciousness supporting networks. *Current Opinion in Neurobiology*, *23*(2), 239–244.

Finn, E. S., Shen, X., Scheinost, D., Rosenberg, M. D., Huang, J., Chun, M. M., … Todd Constable, R. (2015). Functional connectome fingerprinting: Identifying individuals using patterns of brain connectivity. *Nature Neuroscience*, *18*(11), 1664–1611.

Fox, M. D., Halko, M. A., Eldaief, M. C., & Pascual-Leone, A. (2012). Measuring and manipulating brain connectivity with resting state functional connectivity magnetic resonance imaging (fcMRI) and transcranial magnetic stimulation (TMS). *Neuroimage*, *62*, 2232–2243. http://www.ncbi.nlm.nih.gov/pubmed/22465297

Giacino, J., Fins, J. J., Laureys, S., & Schiff, N. (2014). Disorders of consciousness after acquired brain injury: The state of the science. *Nature Reviews. Neurology*, *10*(2), 99–114.

Giacino, J. T., Kalmar, K., & Whyte, J. (2004). The JFK Coma Recovery Scale-Revised: Measurement characteristics and diagnostic utility. *Archives of Physical Medicine and Rehabilitation*, *85*(12), 2020–2029.

Guldenmund, P., Vanhaudenhuyse, A., Sanders, R. D., Sleigh, J., Bruno, M. A., Demertzi, A., … Absalom, A. R. (2017). Brain functional connectivity differentiates dexmedetomidine from propofol and natural sleep. *British Journal of Anaesthesia*, *119*(4), 674–684.

Hashmi, J. A., Loggia, M. L., Khan, S., Gao, L., Kim, J., Napadow, V., … Akeju, O. (2017). Dexmedetomidine disrupts the local and global efficiencies of large-scale brain networks. *Anesthesiology*, *126*(3), 419–430.

Heine, L., Soddu, A., Gómez, F., Vanhaudenhuyse, A., Tshibanda, L., Thonnard, M., … Demertzi, A. (2012). Resting state networks and consciousness alterations of multiple resting state network connectivity in physiological, pharmacological, and pathological consciousness states. *Frontiers in Psychology*, *3*, 1–12.

Hettmansperger, T. P., & McKean, J. W. (2011). *Robust nonparametric statistical methods*. CRC Press.

van den Heuvel, M. P., de Lange, S. C., Zalesky, A., Seguin, C., Yeo, B. T. T., & Schmidt, R. (2017). Proportional thresholding in resting-state fMRI functional connectivity networks and consequences for patient-control connectome studies: Issues and recommendations. *NeuroImage*, *152*, 437–449.

Hollander, M., & Wolfe, D. A. (1999). *Nonparametric statistical methods*. Wiley.

Kloke, J. D., & Mckean, J. W. (2012). Rfit : Rank-based estimation for linear models rank-regression. *The R Journal*, *4*, 57–64.

Mochalova, EG., Legostaeva, L. A., Zimin, AA., Yusupova, D. G., Sergeev, D. V., Ryabinkina, Y. V., ... Piradov, M. A. (2018). Russian version of Coma Recovery Scale-revised (CRS-R) – a standardized method for assessment of patients with disorders of consciousness. Zhurnal Nevrol i Psikhiatrii Im SS Korsakova, in print.

Newcombe, R. G. (1998). Two-sided confidence intervals for the single proportion: Comparison of seven methods. *Statistics in Medicine*, *17* (8), 857–872.

Noirhomme, Q., Brecheisen, R., Lesenfants, D., Antonopoulos, G., & Laureys, S. (2017). Look at my classifier's result": Disentangling unresponsive from (minimally) conscious patients. *NeuroImage*, *145*, 288–303.

Öztürk, F., & Akdeniz, F. (2000). Ill-conditioning and multicollinearity. *Linear Algebra and its Applications*, *321*(1–3), 295–305.

Ripollés, P., Marco-Pallarés, J., de Diego-Balaguer, R., Miró, J., Falip, M., Juncadella, M., ... Rodriguez-Fornells, A. (2012). Analysis of automated methods for spatial normalization of lesioned brains. *NeuroImage*, *60*(2), 1296–1306.

Robin, X., Turck, N., Hainard, A., Tiberti, N., Lisacek, F., Sanchez, J.-C., & Müller, M. (2011). pROC: An open-source package for R and S+ to analyze and compare ROC curves. *BMC Bioinformatics*, *12*, 77.

Rosazza, C., Andronache, A., Sattin, D., Bruzzone, M. G., Marotta, G., Nigri, A., ... Minati, L. (2016). Multimodal study of default-mode network integrity in disorders of consciousness. *Annals of Neurology*, *79* (5), 841–853.

Rosenberg, M. D., Finn, E. S., Scheinost, D., Papademetris, X., Shen, X., Constable, R. T., & Chun, M. M. (2016). A neuromarker of sustained attention from whole-brain functional connectivity. *Nature Neuroscience*, *19*(1), 165–171.

Seel, R. T., Sherer, M., Whyte, J., Katz, D. I., Giacino, J. T., Rosenbaum, A. M., ... Zasler, N. (2010). Assessment scales for disorders of consciousness: Evidence-based recommendations for clinical practice and research. *Archives of Physical Medicine and Rehabilitation*, *91*(12), 1795–1813.

Shen, X., Tokoglu, F., Papademetris, X., & Constable, R. T. (2013). Groupwise whole-brain parcellation from resting-state fMRI data for network node identification. *NeuroImage*, *82*, 403–415.

Silva, S., De Pasquale, F., Vuillaume, C., Riu, B., Loubinoux, I., Geeraerts, T., ... Peran, P. (2015). Disruption of posteromedial large-scale neural communication predicts recovery from coma. *Neurology*, *85*(23), 2036–2044.

Soddu, A., Vanhaudenhuyse, A., Bahri, M. A., Bruno, M. A., Boly, M., Demertzi, A., ... Noirhomme, Q. (2012). Identifying the default-mode component in spatial IC analyses of patients with disorders of consciousness. *Human Brain Mapping*, *33*(4), 778–796.

Stender, J., Gosseries, O., Bruno, M. A., Charland-Verville, V., Vanhaudenhuyse, A., Demertzi, A., ... Laureys, S. (2014). Diagnostic precision of PET imaging and functional MRI in disorders of consciousness: A clinical validation study. *Lancet (London, England)*, *384*(9942), 514–522.

Vanhaudenhuyse, A., Noirhomme, Q., Tshibanda, L. J. F., Bruno, M. A., Boveroux, P., Schnakers, C., ... Boly, M. (2010). Default network connectivity reflects the level of consciousness in non-communicative brain-damaged patients. *Brain*, *133*(1), 161–171.

Wang, J., Zuo, X., & He, Y. (2010). Graph-based network analysis of resting-state functional MRI. *Frontiers in Systems Neuroscience*, *4*, 16.

Whitfield-Gabrieli, S., & Nieto-Castanon, A. (2012). *Conn*: A functional connectivity toolbox for correlated and anticorrelated brain networks. *Brain Connect*, *2*(3), 125–141.

Wu, X., Zou, Q., Hu, J., Tang, W., Mao, Y., Gao, L., ... Yang, Y. (2015). Intrinsic functional connectivity patterns predict consciousness level and recovery outcome in acquired brain injury. *Journal of Neuroscience*, *35*(37), 12932–12946.

Yeo, B. T. T., Krienen, F. M., Sepulcre, J., Sabuncu, M. R., Lashkari, D., Hollinshead, M., ... Buckner, R. L. (2011). The organization of the human cerebral cortex estimated by intrinsic functional connectivity. *Journal of Neurophysiology*, *106*, 1125–1165.

Zheng, Z. S., Reggente, N., Lutkenhoff, E., Owen, A. M., & Monti, M. M. (2017). Disentangling disorders of consciousness: Insights from diffusion tensor imaging and machine learning. *Human Brain Mapping*, *38* (1), 431–443.

**How to cite this article:** Sinitsyn DO, Legostaeva LA, Kremneva EI, et al. Degrees of functional connectome abnormality in disorders of consciousness. *Hum Brain Mapp*. 2018;00:1–12. https://doi.org/10.1002/hbm.24050